SEISMOLOGICAL STUDIES OF GEOTHERMAL SYSTEMS IN THE TAUPŌ VOLCANIC ZONE

Martha Savage[1], John Townend[1], Steven Sewell[1], Chet Hopp[1], Stefan Mroczek[1,2], Francesco Civilini[1,3], Brook Keats[1,4]

[1]SGEES, Victoria University of Wellington, Wellington, New Zealand

[2]Now at: GFZ German Research Centre for Geosciences, Potsdam, Germany and Freie University Berlin, Germany

[3]Now at: USGS, Menlo Park, California, USA

[4]Now at: Worcester College, University of Oxford, UK

Martha.Savage@vuw.ac.nz

Keywords: *Microseismicity, Anisotropy, Brittle-ductile transition, Ambient noise, Temporal variations*

ABSTRACT

In the last decade, in partnership with Mercury NZ Limited (formerly Mighty River Power), Victoria University of Wellington postgraduate students have used seismic data from New Zealand's geothermal fields to elucidate the structure and geomechanical properties of several geothermal systems in the Taupō Volcanic Zone. Recent projects have focussed on the Rotokawa and Ngatamariki fields, but earlier studies looked at Kawerau.

Double difference earthquake locations reveal that under Kawerau the majority of seismicity is shallower (4 km maximum depth) than in the surrounding regions (6-7 km). This suggests that the major heat source is situated beneath the centre of the field and that at levels deeper than 4 km the ground is too hot to support brittle failure.

Between 2012 and 2015, matched filter methods doubled the number of earthquakes detected in Rotokawa and Ngatamariki to about 9000. The focal mechanisms of almost 1000 of those events were inverted to determine the prevailing stress field. At Ngatamariki, the new locations exhibit a strong spatio-temporal association with borehole drilling and stimulation. Areas of high b-values (a measure of the ratio of the numbers of small to large earthquakes) correspond to areas of elevated pore fluid pressure and a broad distribution of fractures. Focal mechanism inversion yields a normal faulting stress state with a NW/SE axis of minimum compressive stress (S_3), but distinct regions vary from the average. Shear wave splitting also yields NE/SW fast directions, consistent with the presence of stress-aligned cracks and NW/SE extension. Changes in delay time and Vp/Vs ratios correlate with changing volumes of production. Changes in isotropic shear velocity were measured from stacking noise cross-correlations. There were faster velocities in regions of injection, and gradual increases in shear-wave velocity from 0.06% to 0.08% over a year, but it remains difficult to distinguish the effects of rainfall changes and production. We observed abrupt decreases in velocity by as much as 0.07% in Ngatamariki immediately after regional and local earthquakes, which returned to normal over a period of several weeks.

1. INTRODUCTION

1.1 Background

Earthquake sensors have been installed in many geothermal areas to monitor background seismicity and warn of changing conditions that might lead to larger earthquakes. However, the data collected by these microseismic sensors may also be used to provide important information on the reservoirs including identifying major structures, monitoring changes in reservoir properties and characterizing stress state. This information can be used for constructing reservoir models, which are then used to optimize production and injection strategies and to explore further development of the fields. To pursue these latter goals, Mercury NZ Limited has funded scholarships at Victoria University of Wellington. These have led to better understanding of 1) the depth of the brittle-ductile transition, which is related to temperature at depth; 2) the local stress field; 3) the relation between reservoir injection, extraction and pressures and changes in microseismicity, isotropic and anisotropic velocity (and hence reservoir crack properties) with time. Here we provide a review of our results and suggest new avenues for future work.

1.2 Tectonic setting and geothermal production history

All three of the geothermal fields that we have studied are in the Taupō Volcanic Zone, a region of high heat flow (Wilson et al., 1995) formed in the back arc of the subducting Pacific Plate along the Hikurangi Margin (Figure 1)

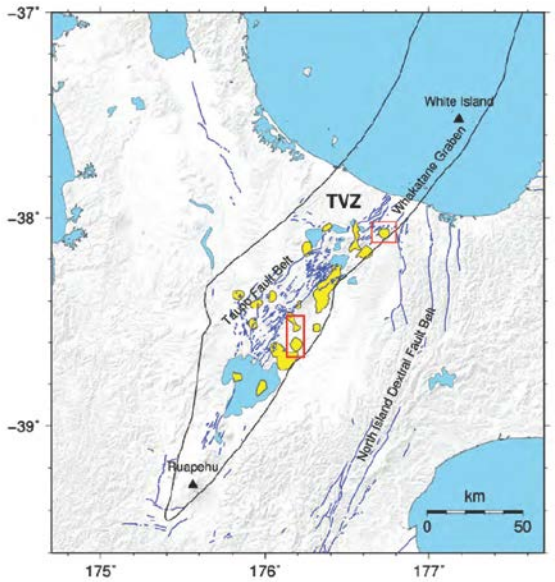

Figure 1. Geothermal fields (yellow) in the Taupō Volcanic Zone (TVZ) of New Zealand (Bibby et al., 1995). The black lines mark the young TVZ boundary (Wilson et al., 1995). Blue lines are faults from the GNS Fault map database (Litchfield et al., 2014). Red boxes mark the fields used in this paper. Kawerau is in the NE, Ngatamariki is the northernmost field in the SW box, and Rotokawa is the southernmost field in the SW box.

Geothermal power and direct use operations started at Kawerau in 1957 and more than 70 wells have been drilled since then (Milicich et al., 2016). An array of 1 Hz seismometers has operated continuously in the field from 2008 (Keats, 2014; Rawlinson et al., 2012). Production at Rotokawa began in 1997 and was expanded in 2010. Temporary seismic networks installed in 2005 and 2006 were followed by a permanent network of 10 seismometers that has

been in operation since 2008 (Sherburn et al., 2015). A seismic monitoring array of 12 seismometers, including three downhole seismometers, was installed at Ngatamariki in 2012, approximately one year prior to the start of production at the field.

Prior to the research presented here, VUW MSc student Daniel Clarke used GeoNet data to study the seismicity and velocity structure of Kawerau (Clarke, 2008; Clarke et al., 2009). VUW MSc student Zara Rawlinson used matched filter methods to study swarms of earthquakes in the Rotokawa field and developed a method to determine how best to place new seismometers in an area, which was used to deploy the Kawerau network (Rawlinson, 2011; Rawlinson et al., 2012). Finally, MSc student Gabe Matson developed a matched filter method to study Ngatamariki (Matson, 2016), which was further developed by Chet Hopp (Hopp, 2019; Hopp et al., 2019a).

2. DATA AND METHODS

We used records from seismometers located in all three fields (Figure 2 & 3).

2.1 Location methods

For all fields we started with hypocentres computed initially by GNS Science, under contract to Mercury. Because the Ngatamariki and Rotokawa fields are so close, the records from both fields are combined to analyse them together.

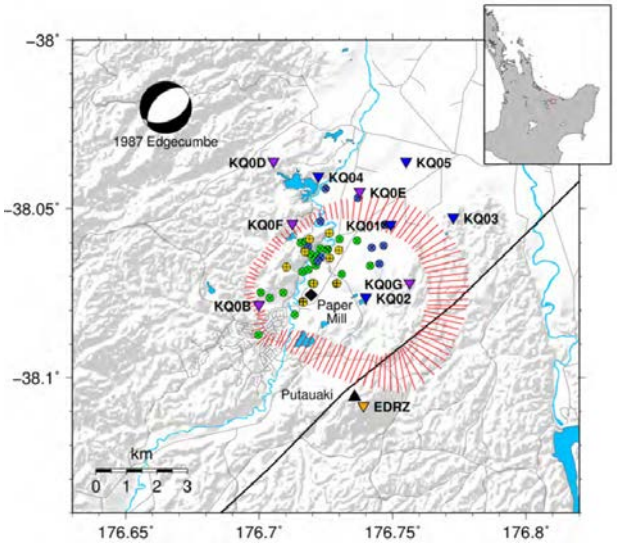

Figure 2. The Kawerau Geothermal Field. The red lines represent the boundary of the field from resistivity surveys (Allis et al., 1993). Seismometers are inverted triangles. Gold, blue and green crossed circles represent production, re-injection and monitoring wells respectively. The focal mechanism of the 1987 ML=6.3 Edgecumbe earthquake is shown (Anderson and Webb, 1989), although the earthquake occurred outside the study area. The locations of the Kawerau pulp and paper mill and Putauaki volcano are marked with the diamond and triangle respectively and the eastern boundary of the TVZ is shown by the black line.

2.1.1 Kawerau locations

Details of the procedure to locate the Kawerau earthquakes are in Keats (2014), which was based in part on earlier work (Clarke et al., 2009; Rawlinson et al., 2012). Waveforms recorded at the Kawerau stations illustrated in Figure 2 were extracted around the GeoNet earthquake times between 1 Jan. 2008 and 30 June 2013. P and S arrival times and initial polarities were determined manually and preliminary locations were computed with the nonlinear location program Nonlinloc (Lomax et al., 2009). Waveform cross-correlation methods (Du et al., 2004) were then used to determine high-precision arrival times and the earthquake locations were refined with the HYPODD code, which uses the double-difference method of Waldhauser and Ellsworth (2000).

2.1.2 Ngatamariki and Rotokawa locations

Details of the procedures used to locate earthquakes within the Ngatamariki and Rotokawa fields have been documented by (Hopp, 2019); Hopp et al. (2019a). Earthquakes located for Mercury by GNS Science between 15 May 2012 and 18 November 2015 within or near the Ngatamariki and Rotokawa fields were used as "templates" to find smaller events with similar waveforms (and therefore locations and focal mechanisms). Cross-correlating the waveforms of the templates with continuous seismic records by the EQcorrscan technique (Chamberlain et al., 2017) found smaller events within the noise. Cross-correlation methods were also used to pick P arrival times, and events with more the five P picks were used to determine S arrivals via an automatic picking program (Castellazzi et al., 2015; Diehl et al., 2009). Using this set of arrival times, Nonlinloc was used to locate the earthquakes and the initial hypocenters were refined by the double-difference relocation program GrowClust (Trugman and Shearer, 2017).

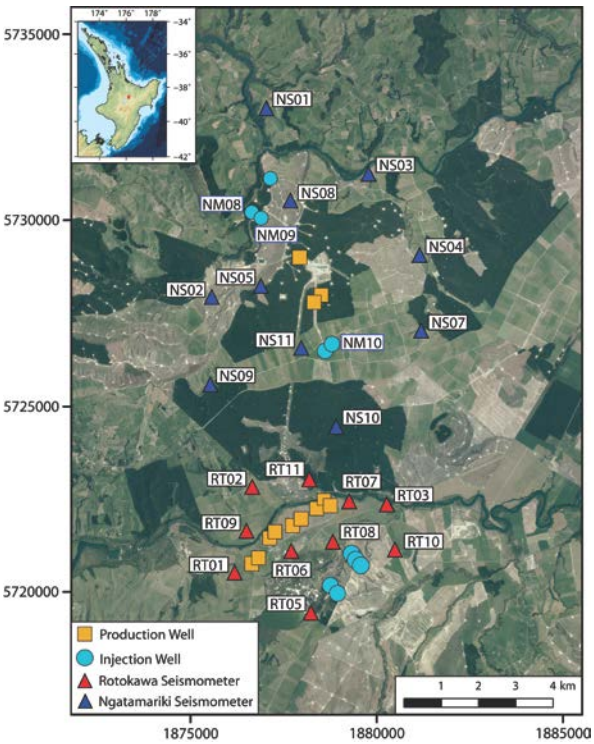

Figure 3. Map of seismometers (triangles), injection wells (circles), and production wells (squares) operated by Mercury Energy at Rotokawa from 2009-2010 and Ngatamariki from 2012-2013. Coordinates are New Zealand Transverse Mercator 2000 (NZTM2000) (Civilini, 2018; Civilini et al., 2019).

2.2 Focal Mechanisms and stress inversion

Focal mechanisms were determined from first-motion polarities using a Bayesian method (Walsh et al., 2009). The focal mechanisms were inverted for stress field orientation and stress ratio using another Bayesian algorithm (Arnold and Townend, 2007), which takes imprecise knowledge of

velocity structure and observational errors into account when computing posterior uncertainties.

2.3 Shear Wave Splitting and Vp/Vs ratio

S arrivals from the picking described above at Ngatamariki and Rotokawa were used to calculate shear wave splitting fast directions and delay times using the MFAST code (Savage et al., 2010). Full details are described by Mroczek (2017); (Mroczek et al., 2019). Fast orientations give an estimate of the orientation of anisotropy and delay times represent the accumulation of the effects of anisotropy along the ray path from an earthquake (source) to a seismometer (receiver). Near-surface anisotropy is usually dominated by cracks, in which case the fast directions represent the orientation of preferentially aligned (usually vertical) cracks. These cracks are in turn oriented parallel to the maximum horizontal stress direction, SHmax (Nur and Simmons, 1969). Delay times depend on the aspect ratios of the cracks, their density within the volume, and the material filling the cracks (e.g., liquid or gas)(Hudson, 1981).

The P- and S- arrival times (Tp and Ts, respectively) from the highest-quality shear wave splitting measurements were also used to calculate the Vp/Vs ratios (Nur, 1972).

2.4 Isotropic velocity changes

We used the MSNOISE package (Lecocq et al., 2014) to calculate cross-correlation functions and velocity changes based on the Moving-window cross spectrum (MWCS) technique (Clarke et al., 2011; Ratdomopurbo and Poupinet, 1995). Cross-correlation functions are calculated by adding together (stacking) waveforms determined by cross-correlating long records of noise between pairs of seismometers. The superposition of waves in the stacked signals reveals coherent seismic waves traveling between the two stations, as if one station acts as a source while the other is a receiver (Shapiro and Campillo, 2004). Waves traveling along other directions are not in phase and are therefore attenuated in the final stack. Surface waves are the dominant waves in the direct signal, and scattered waves are recorded after the direct arrivals. Seismic velocity is sensitive to variations in the elastic properties of the wave field. Scattered waves arriving at increasing times after the direct arrivals have travelled progressively further, and are therefore increasingly affected by any changes in seismic velocity in the area (Brenguier et al., 2008b). These changes result in

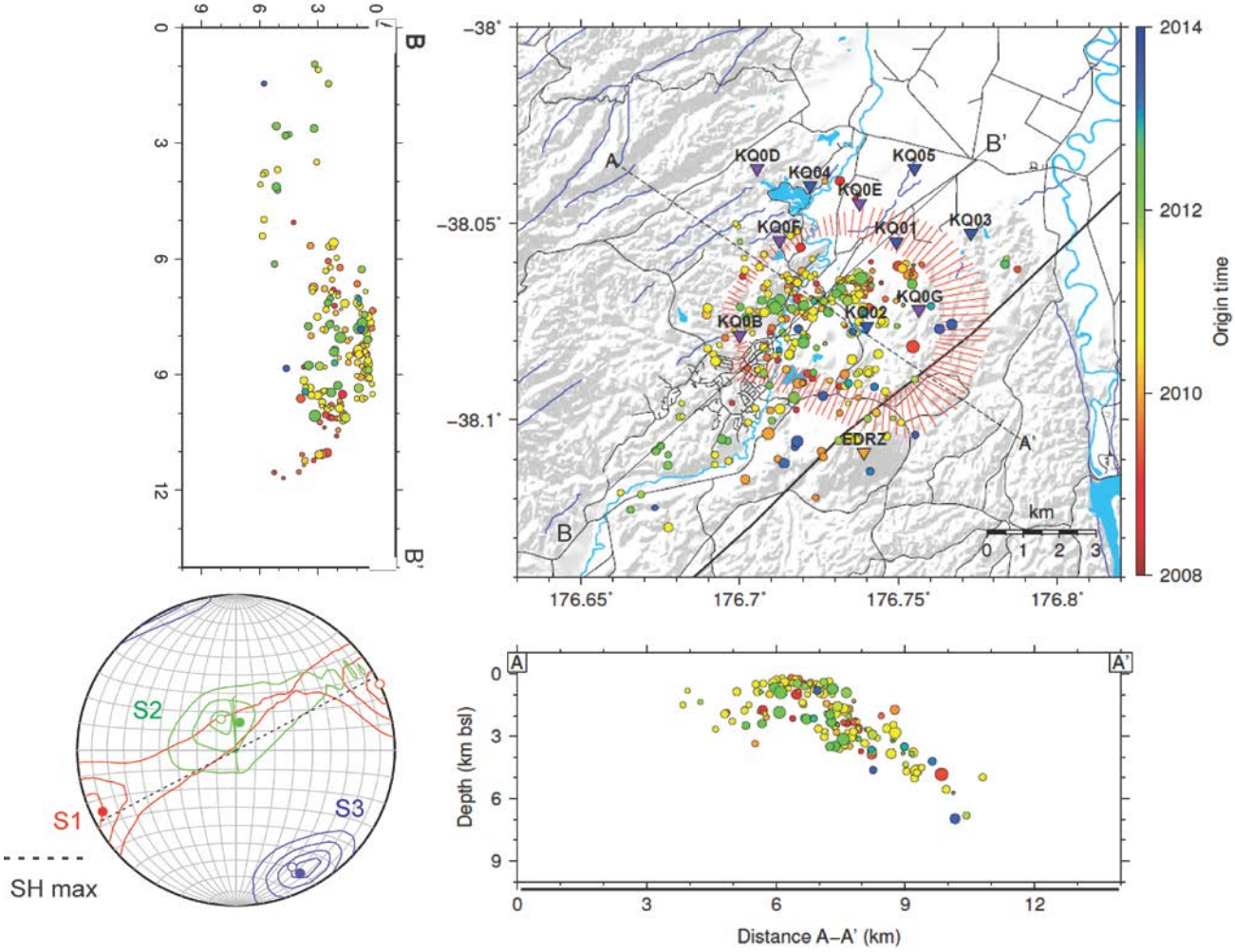

Figure 4. Map and cross-section view of final locations in Kawerau. Colours represent origin time. Other symbols are as in Figure 2.Bottom Left: Stress tensor inversion for the 14 Kawerau earthquakes. S1=maximum principal stress, S2=intermediate principal stress, S3=minimum principal stress, SH max = maximum horizontal stress.

later or earlier arrivals, with phase delays or advances between stacked waveforms recorded over different time periods. Changes in fluid pressure and saturation, fluid content, rock stress or crack numbers can change the velocity in the medium, and therefore this technique could help to monitor changing reservoir conditions.

3. RESULTS AND DISCUSSION

3.1 Microearthquake locations and stress determinations

3.1.1 Kawerau locations and stress

Figure 4 shows the final 281 Kawerau earthquake locations from the double-difference technique in a map view and with two perpendicular cross sections (Keats, 2014). The maximum earthquake depths are much shallower under the center of the geothermal field (~ 3–5 km) than either within the TVZ to the southwest (6 km) or to near the western edge of the TVZ (8 km).

The shallower locations could be caused by a higher temperature under the field. Generally above a temperature of about 350° C earth materials cannot support brittle failure and deform in a ductile fashion. This is consistent with the high temperatures report in the Kawerau field of up to 310°C (Bignall and Harvey, 2005). However, another hypothesis is that the shallow earthquakes in the field are caused by fluid movements associated with the geothermal production and that deeper seismicity is simply absent because any seismogenic structures at those depths were not active during the time period under investigation.

Focal mechanisms were obtained for 14 events, which exhibited strike-slip and normal mechanisms. Using these to invert for the stress tensor yields a strike-slip to normal faulting stress state with an SHmax direction of 65° (Figure 4). This is consistent with other estimates of extension in the TVZ (Milicich et al., 2013; Townend et al., 2012)

3.1.2 Seismicity in Rotokawa and Ngatamariki

The ~9000 earthquake locations in both the Rotokawa and Ngatamariki geothermal fields are generally associated with production and injection wells (Figure 5, 6)(Hopp, 2019; Hopp et al., 2019b). However, the maximum depths are shallower at Ngatamariki, mostly at or above the bottom of the injection wells (3 km). They are mainly confined within one km horizontally of the wells (Figure 5). At Rotokawa, earthquake depths generally exceed the well depths of 3 km (Figure 6) and the seismicity occurs in a cloud adjacent to injection wells but offset towards production by approximately 2 km. The southeastern seismicity may be bounded by a curved Central Field Fault. Well-constrained focal mechanisms at Ngatamariki (205) and Rotokawa (777) were used to invert for stress state. The stress state was mostly as expected for the TVZ, with normal faulting or strike-slip stress regimes and SHmax broadly NE/SW. However, in northwest Ngatamariki near an intrusion, the stress state appears to rotate with no principal stress axis vertical (Hopp, 2019).

The slope of a Gutenberg-Richter plot, or b-value, is greater than 1 when there are more small earthquakes than usual, which may correspond to areas of high pore-fluid pressure and less than 1 when there are more large earthquakes than usual. Figure 6 shows that the b-values exceed 1 under the injection wells, fitting the hypothesis of high b-values for high pore-fluid pressures. They are less than 1 near the production wells (Hopp, 2019; Hopp et al., 2019b).

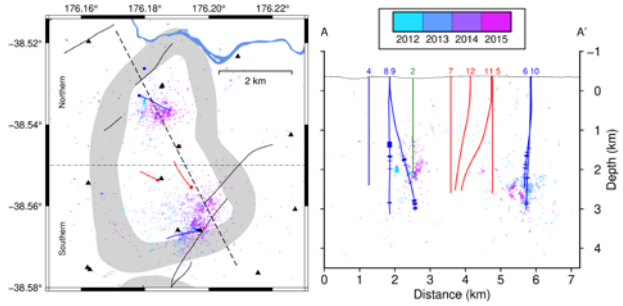

Figure 5. Seismicity at Ngatamariki from May 2012-November 2015. Colours represent time. Black lines are faults, black triangles are seismometer locations), blue lines are injection wells and red lines are production wells.

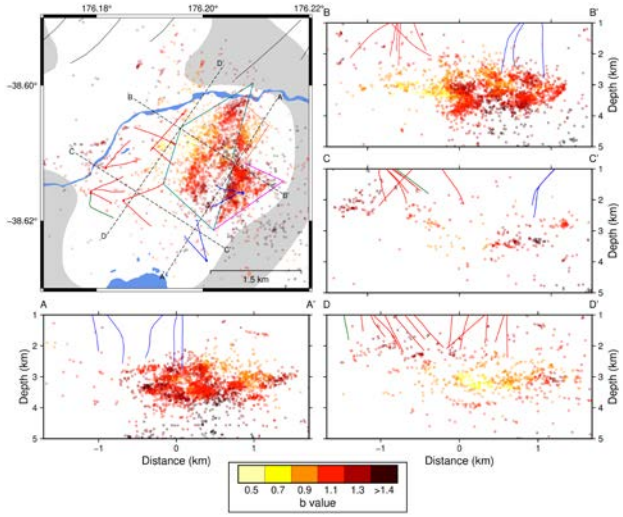

Figure 6. Rotokawa seismicity from 2012-2015 coloured by b-value of the nearest 300 events(Hopp et al., 2019b). Four cross sections show the depth distribution of seismicity. The dashed diamond indicates a previously identified area of dense seismicity (Sherburn et al., 2015).

Installing seismometers approximately one year before the production at Ngatamariki allowed detailed comparisons between drilling, stimulation and the onset of large-scale production/injection with microearthquake activity (Figure 7). Injectivity increases are thought to reflect opening of fractures. Yet earthquakes did not start until about 10 days after the start of injection. We infer that the initial injectivity increase was caused by aseismic thermal rock contraction (Grant et al., 2013). The delay in the earthquake occurrence is thought to be due to near-field (NF) pressurisation of the reservoir followed by pressure breakthrough (BT) to a highly permeable fracture zone. Earthquakes stopped as soon as the injection stopped (end of FZ1) and the wellhead pressure fell to zero. Renewed stimulation from 1 July resulted in a few very small magnitude earthquakes, with higher numbers of earthquakes once the well head pressure was increased four days later (FZ2). Drilling losses while well NM10 was drilled also resulted in increased seismicity, more so than later tests of injection and stimulation, indicating that significant induced seismicity can occur purely through the drilling process (Hopp et al., 2019a).

3.2 Shear wave splitting and seismic anisotropy results

Spatially averaged fast orientations, which should correspond to SHmax if controlled by crack closure, are shown in Figure 8 for Ngatamariki and Rotokawa. They tend to be NE/SW, as expected for extension perpendicular to the strike of the TVZ. These values of SHmax are also consistent with inversions of

focal mechanisms here (Section 3.12) and at Kawerau (Figure 4, section 3.1.1), in the TVZ in regional studies (Townend et al., 2012), and with borehole breakouts in Rotokawa (McNamara et al., 2015).

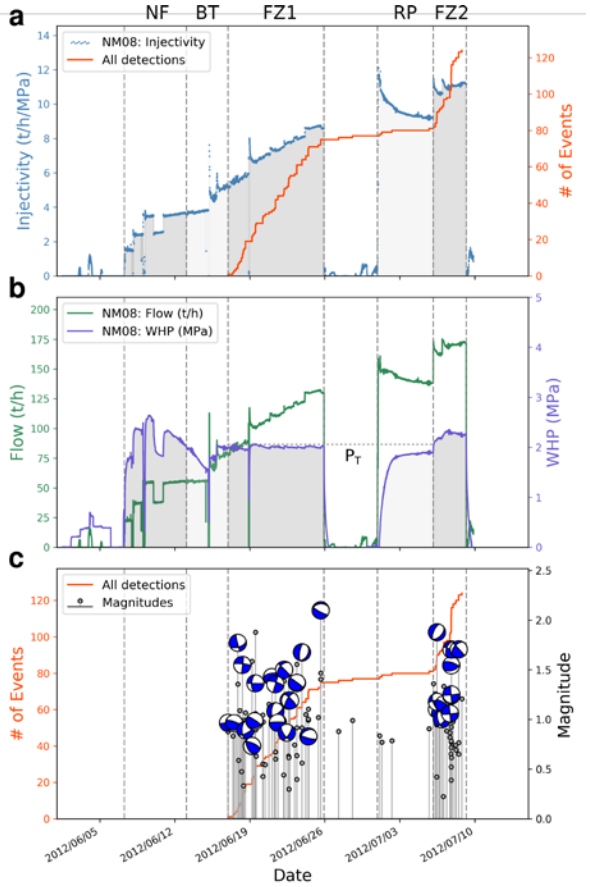

Figure 7. Microearthquake response to cold water stimulation at Ngatamariki well NM08 as a function of time (Hopp et al., 2019a). a) Cumulative seismicity and injectivity; b) Flow rate and well head pressure; c) earthquake magnitudes and focal mechanisms.

The start-up of the Ngatamariki plant correlated to an increase in percent anisotropy (Figure 9), which we attribute to increased fracturing related to the increased seismicity. The increase in anisotropy lags the increase in seismicity, but a slow decrease in anisotropy accompanies the later decrease in seismicity.

3.3 Isotropic velocity changes

Isotropic velocity changes averaged over the Ngatamariki field yield apparent seasonal variations, with velocity 0.08 % higher in autumn (March-June) than in spring (September-November) (Figure 10). In studies elsewhere, higher groundwater levels tend to results in decreased shear velocity through saturation of fractures (e.g., Meier et al., 2010), but here the higher groundwater levels occur slightly earlier than the lowest velocity variations. Earthquakes also seem to temporarily decrease the seismic velocity (Figure 10). A magnitude 5.5 earthquake 3 km away and the two Cook Strait M=6.5 earthquakes over 350 km away all give similar velocity decreases of -0.03% to -0.07% and recover with over similar time frames. Such changes with seismic velocity after the passage of earthquakes have been increasingly observed over the last ten years (Brenguier et al., 2008a; Heckels et al., 2018) and may be particularly pronounced in volcanic or geothermal regions (Brenguier et al., 2014; Yates et al., 2019). These decreases may be caused by different mechanisms for nearby earthquakes, where fracturing may be dominant, and distant earthquakes in which poroelastic

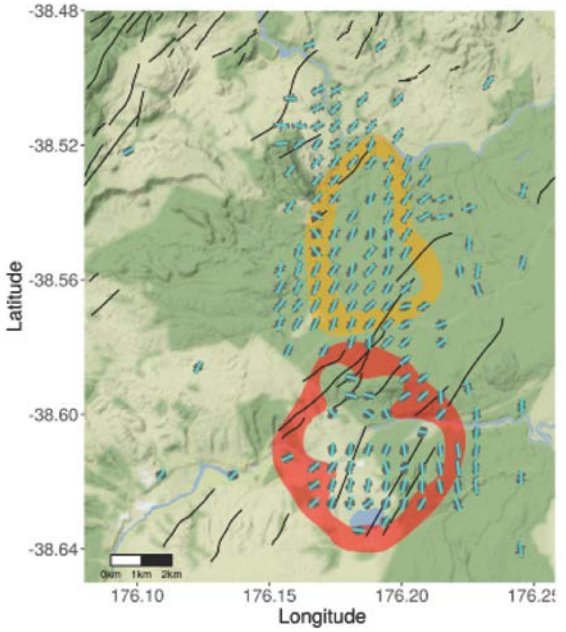

Figure 8. Spatial average of shear-wave splitting fast directions using a regular grid. The outlines of geothermal fields Ngatamariki is in yellow and Rotokawa is in red. Each grid contains a result only if there was a significant orientation. Black lines are faults. From (Mroczek et al., 2019)

changes may cause the observed velocity decreases. Although some evidence suggests that velocity increases near to injection areas when they start up (Civilini, 2018), the seasonal effects need to be corrected before quantitative comparisons can be made.

4. CONCLUSIONS AND SUGGESTIONS FOR FUTURE WORK

Seismic techniques have potential to add another dimension to monitoring in geothermal reservoirs. Knowledge of the stress field can help to determine where drilling and production will be most effective. We suggest that more geothermal fields in New Zealand and worldwide should be investigated to allow similar comparisons and to help understand the mechanics of the field as well as to help in reservoir management. We also suggest that longer time series be examined across the geothermal fields in New Zealand to determine if the variations and correlations we've seen between production, injectivity, seismicity, and isotropic and anisotropic seismic velocity can be better related and modelled to geothermal production, which will allow them to be further developed as monitoring methods

ACKNOWLEDGEMENTS

Mercury NZ Limited provided the data and scholarships to Keats, Hopp, Sewell, Civilini and Mroczek. Ian Richardson, Rob Holt, John Clark, Steven Sherburn, Sandra Bourguignon, Steven Bannister, Zara Rawlinson, provided helpful discussions. Contact Energy provided data from two

seismometers located near the Rotokawa/Ngatamariki fields. M.S. was partly funded by the New Zealand Ministry of Business, Innovation and Employment (MBIE) ECLIPSE Grant (contract CONT-52100-ENDRP-RSCHTRUSTVIC).

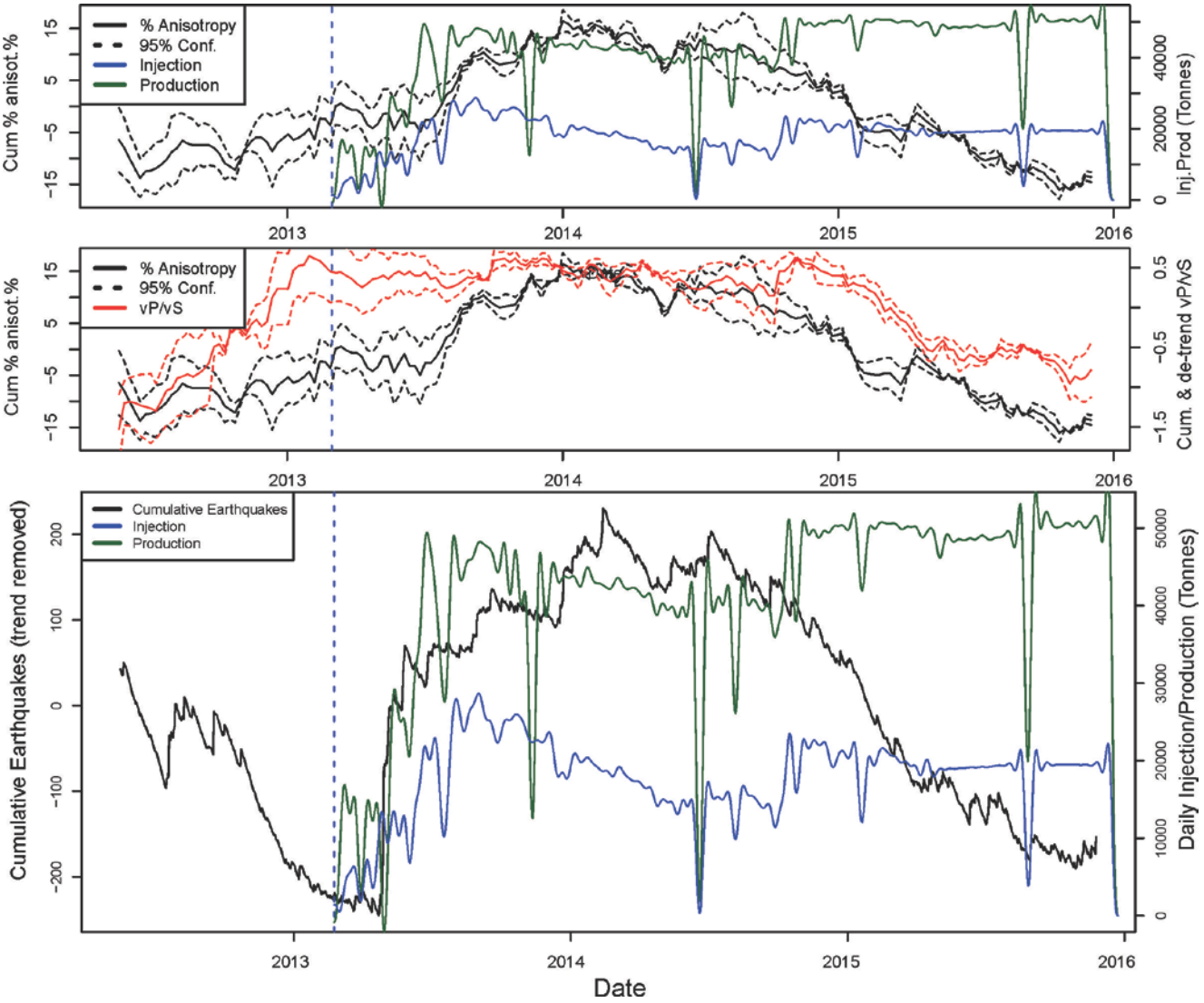

Figure 10. Changes in isotropic velocity at Ngatamariki along with rainfall, groundwater level and flow rates.

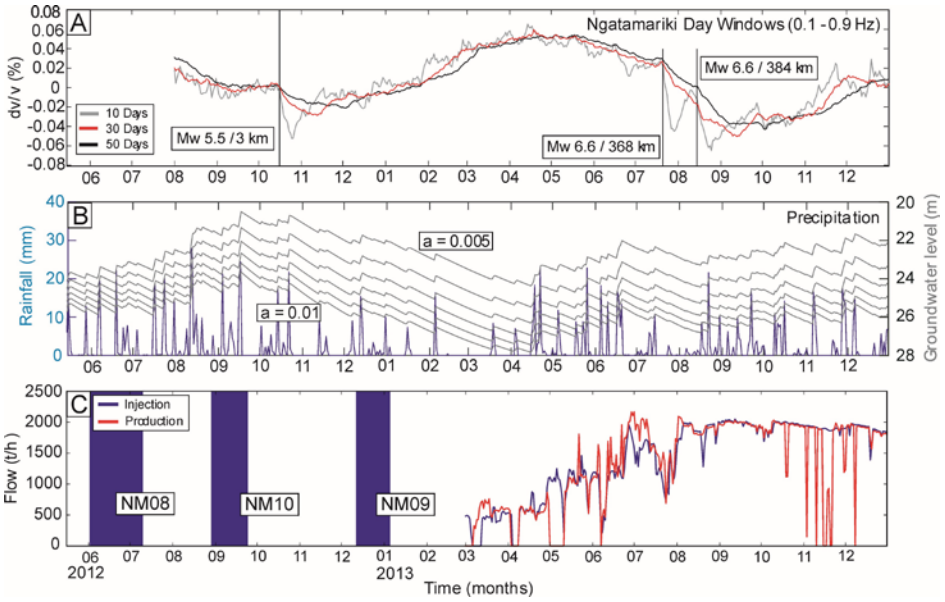

Figure 9. Change over time of cumulative values with trend removed in southern Ngatamariki of (top) percent anisotropy (middle) Vp/Vs and (bottom) microearthquake numbers (Mroczek et al., 2019).

REFERENCES

Allis, R., Christensen, B., Nairn, I. A., Risk, G. F., and White, S., 1993, The natural state of Kawerau geothermal field, Proceedings of the 15th NZ Geothermal Workshop, p. 227-233.

Anderson, H., and Webb, T., 1989, The rupture process of the 1987 Edgecumbe earthquake, New Zealand: New Zealand Journal of Geology & Geophysics, v. 32, no. 1, p. 43-52.

Arnold, R., and Townend, J., 2007, A Bayesian approach to estimating tectonic stress from seismological data: Geophysical Journal International, v. 170, no. 3, p. 1336-1356.

Bibby, H. M., Caldwell, T. G., Davey, F. J., and Webb, T. H., 1995, Geophysical evidence on the structure of the Taupo Volcanic Zone and its hydrothermal circulation: Journal of Volcanology and Geothermal Research, v. 68, no. 1-3, p. 29-58.

Bignall, G., and Harvey, S. D., 2005, Geoscientific review of the Kawerau geothermal field.

Brenguier, F., Campillo, M., Hadziioannou, C., Shapiro, N. M., Nadeau, R. M., and Larose, E., 2008a, Postseismic relaxation along the San Andreas fault at Parkfield from continuous seismological observations: Science, v. 321, no. 5895, p. 1478-1481.

Brenguier, F., Campillo, M., Takeda, T., Aoki, Y., Shapiro, N., Briand, X., Emoto, K., and Miyake, H., 2014, Mapping pressurized volcanic fluids from induced crustal seismic velocity drops: Science, v. 345, no. 6192, p. 80-82.

Brenguier, F., Shapiro, N. M., Campillo, M., Ferrazini, V., Duputel, Z., Coutant, O., and Nercessian, A., 2008b, Towards forecasting volcanic eruptions using seismic noise: Nature Geoscience, v. 1, p. 126-130.

Castellazzi, C., Savage, M. K., Walsh, E., and Arnold, R., 2015, Shear wave automatic picking and splitting measurements at Ruapehu volcano, New Zealand: Journal of Geophysical Research: Solid Earth, v. 120, no. 5, p. 3363-3384.

Chamberlain, C. J., Hopp, C. J., Boese, C. M., Warren-Smith, E., Chambers, D., Chu, S. X., Michailos, K., and Townend, J., 2017, EQcorrscan: Repeating and near-repeating earthquake detection and analysis in Python: Seismological Research Letters., v. in review.

Civilini, F., 2018, Determining seismic shear-velocity from ambient noise sources at regional and local scales [PhD: Victoria University of Wellington, 334 p.

Civilini, F., Savage, M., and Townend, J., 2019, Shear-wave velocity changes induced by earthquakes and rainfall at the Rotokawa and Ngatamariki geothermal fields, Taupo Volcanic Zone, New Zealand: Geophyiscal Journal International, v. submitted manuscript.

Clarke, D., 2008, Velocity modelling and earthquake relocation in the Rotorua and Kawerau geothermal areas, Taupō Volcanic Zone, New Zealand [MSc: Victoria University of Wellington, 188 p.

Clarke, D., Townend, J., Savage, M. K., and Bannister, S., 2009, Seismicity in the Rotorua and Kawerau geothermal systems, Taupo Volcanic Zone, New Zealand, based on improved velocity models and cross-correlation measurements: Journal of Volcanology and Geothermal Research, v. 180, no. 1, p. 50-66.

Clarke, D., Zaccarelli, L., Shapiro, N. M., and Brenguier, F., 2011, Assessment of resolution and accuracy of the Moving Window Cross Spectral technique for monitoring crustal temporal variations using ambient seismic noise: Geophysical Journal International, v. 186, no. 2, p. 867-882.

Diehl, T., Deichmann, N., Kissling, E., and (2009), S. H., 2009, Automatic S-Wave Picker for Local Earthquake Tomography: Bulletin - Seismological Society of America, v. 99, no. 3, p. 1906-1920.

Du, W.-X., Thurber, C. H., and Eberhart-Phillips, D., 2004, Earthquake relocation using cross-correlation time delay estimates verified with the bispectrum method:BSSA v. 94, no. 3, p. 856-866.

Grant, M. A., Clearwater, J., Quinao, J., Bixley, P. F., and Le Brun, M., Thermal stimulation of geothermal wells: a review of field data., *in* Proceedings 38th Workshop on Geothermal Reservoir Engineering, Stanford University, 2013.

Heckels, R. E. G., Savage, M. K., and Townend, J., 2018, Postseismic velocity changes following the 2010 Mw 7.1 Darfield earthquake, New Zealand, revealed by ambient seismic field analysis: Geophysical Journal International, v. 213, no. 2, p. 931-939.

Hopp, C. J., 2019, Characterizing microseismicity at the Rotokawa and Ngatamariki geothermal fields [PhD: Victoria University of Wellington, 218 p.

Hopp, C. J., Sewell, S. M., Mroczek, S., Savage, M., and Townend, J., 2019a, Seismic response to injection well stimulation in a high-temperature, high-permeability reservoir: Geochemistry Geophysics Geosystems, v. 20, p. 2848-2871.

Hopp, C. J., Sewell, S. M., Mroczek, S., Savage, M. K., and Townend, J., 2019b, Seismic response to evolving injection at the Rotokawa geothermal field, New Zealand: Geothermics, v. in revision.

Hudson, J. A., 1981, Wave speeds and attenuation of elastic waves in material containing cracks: Geophysical J. R. Aston. Soc, v. 64, p. 133-150.

Keats, B. S., 2014, A seismological investigation of the Kawerau geothermal field [MSc: Victoria University of Wellington, 83 p.

Lecocq, T., Caudron, C., and Brenguier, F., 2014, MSnoise, a Python package for monitoring seismic velocity changes using ambient seismic noise:

Seismological Research Letters, v. 85, no. 3, p. 715-726.

Litchfield, N., Van Dissen, R., Sutherland, R., Barnes, P., Cox, S., Norris, R., Beavan, R., Langridge, R., Villamor, P., Berryman, K., Stirling, M., Nicol, A., Nodder, S., Lamarche, G., Barrell, D., Pettinga, J., Little, T., Pondard, N., Mountjoy, J., and Clark, K., 2014, A model of active faulting in New Zealand: New Zealand Journal of Geology and Geophysics, v. 57, no. 1, p. 32-56.

Lomax, A., Michelini, A., and Curtis, A., 2009, Earthquake location, direct, global-search methods., Encyclopedia of complexity and system science: New York, Springer Science+Business Media, p. 2449-2473.

Matson, G., 2016, Microseismicity during geothermal stimulation at the Ngatamariki geothermal field: New detections via a matched-filter method [MSc: Victoria University of Wellington, 104 p.

McNamara, D., Massiot, C., Lewis, B. T. R., and Wallis, I. C., 2015, Heterogeneity of structure and stress in the Rotokawa geothermal field, New Zealand: Journal of Geophyiscal Research, Solid Earth, v. 120, no. 2, p. 1243-1262.

Meier, U., Shapiro, N. M., and Brenguier, F., 2010, Detecting seasonal variations in seismic velocities within Los Angeles basin from correlations of ambient seismic noise: Geophysical Journal International, v. 181, no. 2, p. 985-996.

Milicich, S., Wilson, C. J. N., Bignall, G., Pezaro, B., and Bardsley, C., 2013, Reconstructing the geological and structural history of an active geothermal field: A case study from New Zealand: JVGR, v. 262, p. 7-24.

Milicich, S. D., Clark, J. P., Wong, C., and Askari, M., 2016, A review of the Kawerau Geothermal Field, New Zealand: Geothermics, v. 59, p. 252-265.

Mroczek, S., 2017, Seismic anisotropy at the Rotokawa and Ngatamariki geothermal fields in the Taupo Volcanic Zone [MSc: Victoria University of Wellington, 224 p.

Mroczek, S., Savage, M. K., Hopp, C. J., and Sewell, S. M., 2019, Anisotropy as an indicator for reservoir changes: example from the Rotokawa and Ngatamariki geothermal fields, New Zealand: GJI, submitted manuscript.

Nur, A., 1972, Dilatancy, pore fluids, and premonitory variations of t_S/t_P travel times: BSSA, v. 62, no. 5, p. 1217-1222.

Nur, A., and Simmons, G., 1969, Stress-induced velocity anisotropy in rock: an experimental study: J. Geophys. Res., v. 74, p. 6667-6674.

Ratdomopurbo, A., and Poupinet, G., 1995, Monitoring a temporal change of seismic velocity in a volcano: application to the 1992 eruption of Mt. Merapi (Indonesia): GRL, v. 22, no. 7, p. 775-778.

Rawlinson, Z., 2011, Microseismicity associated with actively exploited geothermal systems: earthquake detection and probabilistic location at Rotokawa and statistical seismic network design at Kawerau [MSc: Victoria University of Wellington, 252 p.

Rawlinson, Z. J., Townend, J., Arnold, R., and Bannister, S., 2012, Derivation and implementation of a nonlinear experimental design criterion and its application to seismic network expansion at Kawerau geothermal field, New Zealand: Geophysical Journal International, v. 191, no. 2, p. 686-694.

Savage, M. K., Wessel, A., Teanby, N. A., and Hurst, A. W., 2010, Automatic measurement of shear wave splitting and applications to time varying anisotropy at Mount Ruapehu volcano, New Zealand: Journal of Geophysical Research-Solid Earth, v. 115.

Shapiro, N. M., and Campillo, M., 2004, Emergence of broadband Rayleigh waves from correlations of the ambient seismic noise: Geophysical Research Letters, v. 31, p. 1-4.

Sherburn, S., Sewell, S. M., Bourguignon, S., Cumming, W., Bannister, S., Bardseley, C., Winick, J., Quinao, J., and Wallis, I. C., 2015, Microseismicity at Rotokawa geothermal field, New Zealand, 2008-2012: Geothermics, v. 54, p. 23-34.

Townend, J., Sherburn, S., Arnold, R., Boese, C., and Woods, L., 2012, Three-dimensional variations in present-day tectonic stress along the Australia-Pacific plate boundary in New Zealand: Earth and Planetary Science Letters, v. 353, p. 47-59.

Trugman, D. T., and Shearer, P. M., 2017, GrowClust: A hierarchical clustering algorithm for relative earthquake relocation with application to the Spanish Springs and Sheldon, Nevada, earthquake sequences: Seismological Research Letters, v. 88, no. 2A, p. 379-391.

Waldhauser, F., and Ellsworth, W. L., 2000, A Double-Difference Earthquake Location Algorithm: Method and Application to the Northern Hayward Fault, California: Bulletin of the Seismological Society of America, v. 90, no. 6, p. 1353-1368.

Walsh, D., Arnold, R., and Townend, J., 2009, A Bayesian approach to determining and parametrizing earthquake focal mechanisms: Geophysical Journal International, v. 176, no. 1, p. 235-255.

Wilson, C. J. N., Houghton, B. F., McWilliams, M. O., Lanphere, M. A., Weaver, S. D., and Briggs, R. M., 1995, Volcanic and structural evolution of Taupo Volcanic Zone, New Zealand: a review: Journal of Volcanology and Geothermal Research, v. 68, no. 1-3, p. 1-28.

Yates, A. S., Savage, M. K., Jolly, A. D., Caudron, C., and Hamling, I. J., 2019, Volcanic, co-seismic and seasonal changes detected at White Island (Whakaari) volcano, New Zealand, using seismic ambient noise: GRL, v. 46, no. 1, p. 99-108.